



# Allergologia et immunopathologia

Sociedad Española de Inmunología Clínica,  
Alergología y Asma Pediátrica

[www.all-imm.com](http://www.all-imm.com)



ORIGINAL ARTICLE

OPEN ACCESS 

## Dimethyl itaconate inhibits LPS-induced inflammatory release and apoptosis in alveolar type II epithelial and bronchial epithelial cells by activating pulmonary surfactant proteins A and D

Yun Shi<sup>a</sup>, Huai-qing Yin<sup>b\*</sup>

<sup>a</sup>Shanxi Medical University, Taiyuan, Shanxi, and Department of Pediatrics, Heji Hospital Affiliated to Changzhi Medical College, Changzhi, Shanxi, P.R. China

<sup>b</sup>Department of Pediatrics, First Hospital of Shanxi Medical University, Taiyuan, Shanxi, P.R. China

Received 18 January 2022; Accepted 23 February 2022

Available online 1 November 2022

### KEYWORDS

dimethyl itaconate;  
inflammatory  
release;  
apoptosis;  
pulmonary surfactant  
protein;  
lung injury

### Abstract

**Background:** Injury to the lung is a common, clinically serious inflammatory disease. However, its pathogenesis remains unclear, and the existing treatments, including cytokine therapy, stem cell therapy, and hormone therapy, are not completely effective in treating this disease. Dimethyl itaconate (DMI) is a surfactant with important anti-inflammatory effects.

**Objective:** The present study used alveolar type II (AT II) and bronchial epithelial cells as models to determine the role of DMI in lung injury.

**Material and Methods:** First, the effects of DMI were established on the survival, inflammatory release, and apoptosis in lipopolysaccharide (LPS)-induced AT II and bronchial epithelial cells. The association between DMI and Sirtuin1 (SIRT1) was assessed using molecular docking. Next, by constructing interference plasmids to inhibit surfactant protein (SP)-A and SP-D expressions, the effect of DMI was observed on inflammatory release and apoptosis.

**Results:** The results revealed that DMI increased the survival rate and expression levels of SP-A, SP-D, and SIRT1, and inhibited inflammatory factors as well as apoptosis in LPS-induced cells. Furthermore, DMI could bind to SIRT1 to regulate SP-A and SP-D expressions. After SP-A and SP-D expressions were inhibited, the inhibitory effect of DMI was reversed on inflammatory release and apoptosis.

**Conclusion:** The findings of the present study revealed that DMI inhibited LPS-induced inflammatory release and apoptosis in cells by targeting SIRT1 and then activating SP-A and SP-D. This novel insight into the pharmacological mechanism of DMI lays the foundation for its later use for alleviating lung injury.

© 2022 Codon Publications. Published by Codon Publications.

\*Corresponding author: Dr. Huai-qing Yin, Department of Pediatrics, First Hospital of Shanxi Medical University, 85 Jiefang South Road, Taiyuan, Shanxi 030001, P.R. China. Email address: [yinhuaiqing@yeah.net](mailto:yinhuaiqing@yeah.net)

<https://doi.org/10.15586/aei.v50i6.586>

Copyright: Yun S and Huai-Qing Y

License: This open access article is licensed under Creative Commons Attribution 4.0 International (CC BY 4.0). <http://creativecommons.org/>

## Introduction

Lung injury is a common, clinically serious inflammatory disease<sup>1</sup> characterized by inflammation of the alveoli and lung parenchyma, damage to the alveolar-capillary membrane,<sup>2</sup> increased vascular permeability, and neutrophil recruitment.<sup>3</sup> Its clinical manifestations include severe hypoxemia, pulmonary function changes, pulmonary edema, and respiratory failure.<sup>4,4</sup> When the oxygenation index is <200, the disease is termed acute respiratory distress syndrome (ARDS).<sup>5</sup> The etiology of lung injury is complicated. After ~50 years of research, significant progress has been made toward its treatment; however, its pathogenesis remains unclear.<sup>6</sup> The present hypothesis is that pneumonia cells are overactivated to release inflammatory mediators, and inflammatory factors interact with effector cells, leading to an uncontrolled inflammatory response. At present, strategies for the clinical treatment of lung injury include cytokine therapy, stem cell therapy, and hormone therapy. However, morbidity and mortality from lung injury remain high, particularly for critically ill patients. Lung injury can also be induced by ventilators<sup>7, 8</sup> and radiation therapy,<sup>9</sup> ultimately leading to multiple organ dysfunction. The existing treatments are not completely effective,<sup>10</sup> rendering the identification of new treatments necessary.

Pulmonary surfactant proteins (SP)-A and SP-D belong to the c-type lectin subgroups of the collectin family, which are primarily synthesized and secreted by alveolar type II (AT II), nonciliated bronchial, and bronchiolar epithelial cells.<sup>11</sup> When the lung is damaged, resident epithelial stem cells proliferate and differentiate swiftly to maintain the structure and function of the lung. AT II cells, a type of alveolar structural cells, can function as alveolar stem cells, as they can differentiate into AT I cells and self-restore. Their abnormal proliferation and regulation can result in serious lung diseases.<sup>12</sup> Since the bronchus and lung are closely linked, bronchial biopsy can be used to detect lung injury; therefore, bronchial epithelial cells are also useful in the study of lung injury. In addition, SP-A and SP-D exert a variety of tissue-specific immunomodulatory effects in host defense and physiological state maintenance of various extrapulmonary tissues and organs, such as the nasal cavity.<sup>13</sup> SP-A and SP-D can not only maintain the integrity of epithelial cells but also reduce inflammatory release and apoptosis in the lung.<sup>14</sup> Therefore, the activation and maintenance of SP-A and SP-D have an important protective effect on lung injury and ARDS. In addition, a previous study indicated that Sirtuin1 (SIRT1) activator could up-regulate SP-A expression to relieve emphysema.<sup>15</sup>

Dimethyl itaconate (DMI), as a membrane-permeable derivative of itaconate, is a surfactant with important anti-inflammatory effects. Studies have demonstrated that it can suppress the growth of *Aspergillus fumigatus* and prevent fungal keratitis by activating nuclear factor, erythroid 2 (NF-E2)-related factor-2/heme oxygenase-1 signaling.<sup>16</sup> DMI has been indicated to restrict the inflammatory response of activated macrophages, reduce the production of reactive oxygen species, and alleviate cardiac ischemia/reperfusion injury. In addition, it can inhibit the toxic transformation of microglia around the infarction, which means that it can also play a role in cerebral

ischemia/reperfusion injury.<sup>17</sup> Furthermore, DMI can reduce the secretion of pro-inflammatory cytokines, such as IL-6 and IL-12, and alleviate lipopolysaccharide (LPS)-induced mastitis in mice.<sup>18</sup>

Lipopolysaccharide is an important structural component of the outer membrane of the cell wall of Gram-negative bacteria and one of the most effective known immunostimulants in nature.<sup>19</sup> It is already very common to utilize LPS to establish an inflammation model. The present study used LPS to induce AT II and bronchial epithelial cells to study the effects of DMI on inflammatory cells and explore its mechanism.

## Materials and Methods

### Cell culture and reagents

The human adenocarcinoma A549 cell line was used as an *in vitro* model of type II alveolar epithelium because of its general morphology being similar to type II alveolar epithelial cells.<sup>20</sup> A549 and human bronchial epithelial cells (HBEC) bronchial epithelial cells were purchased from the American Type Culture Collection (USA). Cells were cultured in Dulbecco's Modified Eagle Medium (DMEM) containing 10% fetal bovine serum (FBS) (both bought from Solarbio Co. Ltd., Beijing, China) and 1% penicillin-streptomycin, and maintained in an incubator with 5% carbon dioxide (CO<sub>2</sub>) at 37°C.

Briefly, the two types of cells were separately divided into the following five groups: (i) control; (ii) LPS; (iii) LPS + DMI (0.25 mM); (iv) LPS + DMI (0.5 mM); and v) LPS + DMI (1 mM). In order to detect the relationship between DMI, SP-A, and SP-D via functional experiments, the following six groups were formed: (i) control; (ii) LPS; (iii) LPS + DMI (1 mM); (iv) LPS + DMI (1 mM) + short hairpin (sh)RNA-negative control (NC); (v) LPS + DMI (1 mM) + shRNA-SP-A; and (vi) LPS + DMI (1 mM) + shRNA-SP-D. LPS (10 µg/mL (Beyotime Institute of Biotechnology) was used to treat cells at 37°C for 24 h. Untreated cells were regarded as the control group. Cells in the treatment group were treated with different concentrations of DMI (0.25, 0.5, or 1 mM; Leyan; Shanghai Haohong Biomedical Technology Co. Ltd.) at 37°C for 1 h prior to LPS induction.<sup>16-18</sup> SIRT1 inhibitor, EX527 (5 µM), was purchased from Merck KGaA and incubated with cells for 48 h prior to DMI treatment. The concentration of EX527 was determined using a previous study.<sup>21</sup>

### Cell transfection

A549 and HBEC cells (5 × 10<sup>4</sup> cells/well) were seeded into six-well plates. A total of 2-µg SP-A and 2-µg SP-D shRNA lentiviral vectors (pGPU6/GFP/Neo), and 2-µg non-targeted scrambled control (shRNA-NC) were purchased from Shanghai GenePharma Co. Ltd. Lipofectamine® 2000 (Invitrogen™, Thermo Fisher Scientific Inc.) was used for transfection at 37°C, according to the manufacturer's instructions. Following 48 h of transfection, subsequent experiments were performed. Subsequently, cells were divided into the following six groups: (i) control; (ii) LPS;

(iii) LPS + DMI (1 mM); (iv) LPS + DMI (1 mM) + shRNA-NC; (v) LPS + DMI (1 mM) + shRNA-SP-A; and (vi) LPS + DMI + shRNA-SP-D.

### Molecular docking

The structure of SIRT1 (Protein Data Bank [PDB]: 4Kxq) was downloaded from the Research Collaboratory for Structural Bioinformatics Protein Data Bank (PDB) website (<https://www.rcsb.org>) and analyzed using the PyMOL v2.2.0 software (DeLano Scientific LLC) to remove the excess of water molecules and any irrelevant small ligands carried originally. The chemical structure of DMI was hydrogenated and converted into a MOL2 format file using the OpenBabel v2.2.1 software (<http://openbabel.org/wiki>). Following setting the original ligand position as the docking site, the protein-ligand docking procedure was operated in the AutoDock v4.2 software (Scripps Institute) and the result was displayed automatically.

### Cell counting kit-8 (CCK-8) assay

A549 and HBEC cells ( $5 \times 10^3$ /well) were seeded into 96-well plates and cultured in an incubator containing 5% CO<sub>2</sub> at 37°C overnight. In order to examine the effect of DMI on cell survival, gradient concentrations of DMI (0, 0.1, 0.25, 0.5, or 1 mM) were used to treat cells at 37°C for 24 h. Viable cells were measured after the addition of 10 µL CCK-8 solution at 37°C for another 2 h. For detecting induced cells, LPS and DMI were added together and the same procedure was repeated. Optical density (OD) was measured at a wavelength of 450 nm using a microplate reader (Thermo Fisher Scientific Inc.).

### Enzyme-linked-immunosorbent serologic assay (ELISA)

A549 and HBEC cells ( $5 \times 10^5$ /well) were first digested with trypsin and collected after centrifugation at 300×g for 5 min at room temperature. Following washing with phosphate buffer solution (PBS), the cells were lysed and centrifuged again at 300×g for 10 min at room temperature. The expression of inflammatory factors (tumor necrosis factor- $\alpha$  [TNF- $\alpha$ ], interleukin [IL]-1 $\beta$ , and IL-6) in several groups of A549 and HBEC cells were detected using SimpleStep ELISA® kits (cat. Nos. ab181421, ab229384, and ab178013; Abcam, Cambridge, UK), according to the manufacturer's instructions. OD was measured at 450 nm using the microplate reader.

### Terminal deoxynucleotidyl transferase dUTP nick end labeling (TUNEL) assay

A549 and HBEC cells ( $5 \times 10^5$ /well) were seeded in a 24-well plate and cultured in an incubator with 5% CO<sub>2</sub> at 37°C until they reached 80% confluence. They were then treated with LPS and DMI for 24 h. The cell smears were immersed in fixative solution and fixed for 30 min at room temperature,

followed by washing with PBS. Working fluid was added using an Elabscience® TUNEL assay kit (cat. No. E-CK-A334; Elabscience) according to the manufacturer's instructions. The coverslip was removed, sealed, and observed under a fluorescence microscope (magnification, ×200; Olympus Corporation).

### Western blot analysis

Protein extraction was performed in each group of epithelial cells; a Pierce™ BCA protein assay kit (cat. No. 23225; Thermo Fisher Scientific Inc.) was used for protein quantification. Sodium dodecyl sulfate-polyacrylamide gel electrophoresis (SDS-PAGE) 10% was performed to separate protein samples (25 µg/lane), and the separated protein was then transferred to a polyvinylidene fluoride (PVDF) membrane, followed by incubation in blocking fluid, following washing with tris buffered saline (TBS) and Tween 20 (tris buffered saline with tween [TBST]). The blots were incubated with the following primary antibodies at 4°C overnight: SP-A (cat. No. ab115791; dilution, 1:1000; Abcam), SP-D (cat. No. ab220422; dilution, 1:1000; Abcam), SIRT1 (cat. No. ab32441; 1:20,000; Abcam), Bcl2 (cat. No. ab32124; dilution, 1:1000; Abcam), and Bax (cat. No. ab32503; dilution, 1:1000; Abcam). Following rewashing with TBST, the strips were incubated at room temperature with horseradish peroxidase (HRP)-conjugated anti-rabbit secondary antibody (cat. No. 31461; dilution 1:20,000; Thermo Fisher Scientific Inc.) for 1 h. Enhanced chemiluminescence (ECL) was performed for visualization. Glyceraldehyde 3-phosphate dehydrogenase (GAPDH) was used as a control, and the ImageJ software (v1.8.0; National Institutes of Health) was used for densitometry.

### Reverse transcription-quantitative PCR (RT-qPCR)

Total RNA was isolated from each group of epithelial cells using TRIzol® reagent (Thermo Fisher Scientific Inc.), and complementary DNA (cDNA) was primed using a reverse transcriptase kit (Thermo Fisher Scientific Inc.). The reverse transcription product was diluted and RT-qPCR was performed using a QuantiTect® SYBR Green PCR kit (Qiagen Inc.). Cycling conditions of PCR were as follows: Pre-denaturation at 95°C for 1 min, 40 cycles of 95°C for 12 s and extension at 60°C for 30 s. The 2<sup>- $\Delta\Delta$ C<sub>q</sub></sup> method<sup>22</sup> was used to analyze the data. GAPDH was used for normalization. The primer sequences used for qPCR were as follows: SP-A forward, 5'-AAGCCACTCCACGACTTTAGA-3' and reverse, 5'-GCCCATTGCTGGAGAAGACCT-3'; and SP-D forward, 5'-AGGAGCAAAGGGAGAAAGTGGG-3' and reverse, 5'-CAGCTGTGCCTCCGTAATGG-3'; and GAPDH forward, 5'-GCAAGTTCAACGGCACAG-3' and reverse, 5'-GCCAGTAGACTCCACGACAT-3'.

### Statistical analysis

GraphPad Prism 8.0 (GraphPad Software Inc.) was used for statistical analysis. Data were presented as the mean  $\pm$  SD. Statistical significance was determined through one-way

ANOVA with Tukey's *post hoc* test for comparisons among multiple groups. All experiments were carried out for three times.  $P < 0.05$  was considered as statistically significant.

## Results

### DMI increases the survival of LPS-induced A549 and HBEC cells

Dimethyl itaconate was used to treat cells, and a CCK-8 assay was used to detect the effect of DMI on cell survival. DMI solution was serially diluted, and untreated A549 or HBEC cells were used as control. OD was measured separately in A549 and HBEC cells. All concentrations of DMI had no significant effect on A549 or HBEC cell survival (Figure 1A). The survival rate of the LPS-induced cells was examined. The cells were treated with LPS and different concentrations of DMI at the same time. It was found that the cell survival rate of the LPS group was significantly lower than that of the control group. Furthermore, as the concentration of DMI increased, the cell survival rate also increased compared with the LPS group (Figures 1B and C).

### DMI inhibits inflammatory release in LPS-induced A549 and HBEC cells

Enzyme-linked-immunosorbent serologic assay was performed to detect the expression of inflammatory factors, TNF- $\alpha$ , IL-1 $\beta$ , and IL-6 in the control, LPS-induced, and DMI groups of A549 and HBEC cells. Following treatment with LPS, TNF- $\alpha$ , IL-1 $\beta$ , and IL-6, levels in both A549 and HBEC

cells were significantly elevated compared with the control group. In the DMI group at a concentration of 0.25 mM, a decrease in inflammatory release was observed compared with the LPS group. Following an increase in concentration, this trend became more significant (Figure 2A). The same downward trend was also observed in the release of three inflammatory factors in HBEC cells (Figure 2B).

### DMI inhibits apoptosis in LPS-induced A549 and HBEC cells

In order to study the effect of DMI on epithelial cells, TUNEL staining and Western blotting analyses were used to detect cellular apoptosis. DAPI (4',6-diamidino-2-phenylindole) stained all cells, while TUNEL stained only apoptotic cells. It was observed through fusion that after the cells were induced by LPS, the number of apoptotic cells increased compared with the control group. Following the addition of 0.25-mM DMI, the number of apoptotic cells changed significantly compared with the LPS group. Moreover, when the concentration of DMI was increased to 0.5 or 1.0 mM, the number of apoptotic cells decreased in a dose-dependent manner compared with the LPS group (Figures 3A and B). In addition, the expression levels of B-cell lymphoma-2 (Bcl-2) and Bcl-2-associated X (Bax) in A549 and HBEC cells were determined. It was found that Bcl-2 expression was significantly decreased in the LPS group compared with the control group and then elevated in a concentration-dependent manner after DMI treatment. The expression trend of Bax in each group was the opposite (Figures 3C and D). These results of Western blotting analysis were consistent with those of the TUNEL assay, indicating that DMI may inhibit the apoptosis of LPS-induced epithelial cells.

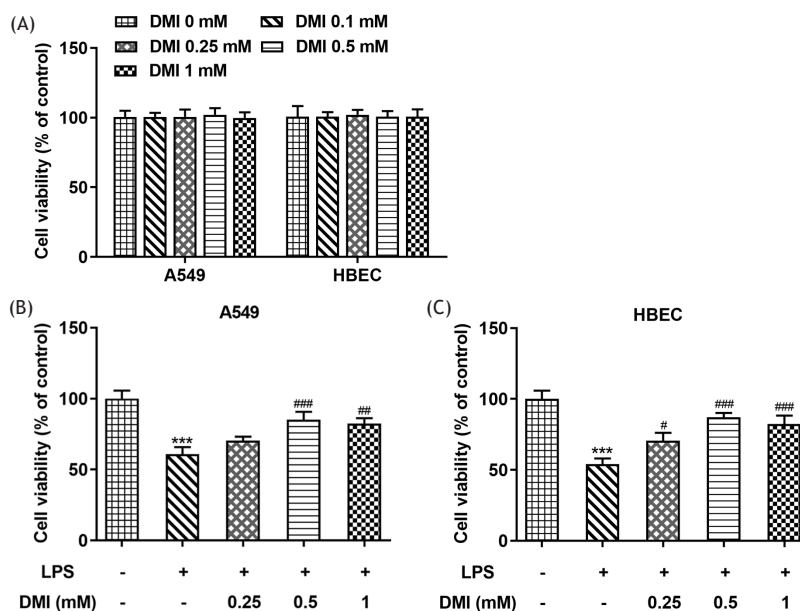


**Figure 1** DMI increases the survival of LPS-induced A549 and HBEC cells. (A) CCK-8 assay was used to detect the effect of different doses of DMI on cell survival. (B) Survival rate of A549 cells induced by LPS and different concentrations of DMI was examined using CCK-8 assay. \*\*\* $P < 0.001$  vs. the control; # $P < 0.05$ , ### $P < 0.01$ , and #### $P < 0.001$  vs. the LPS group.

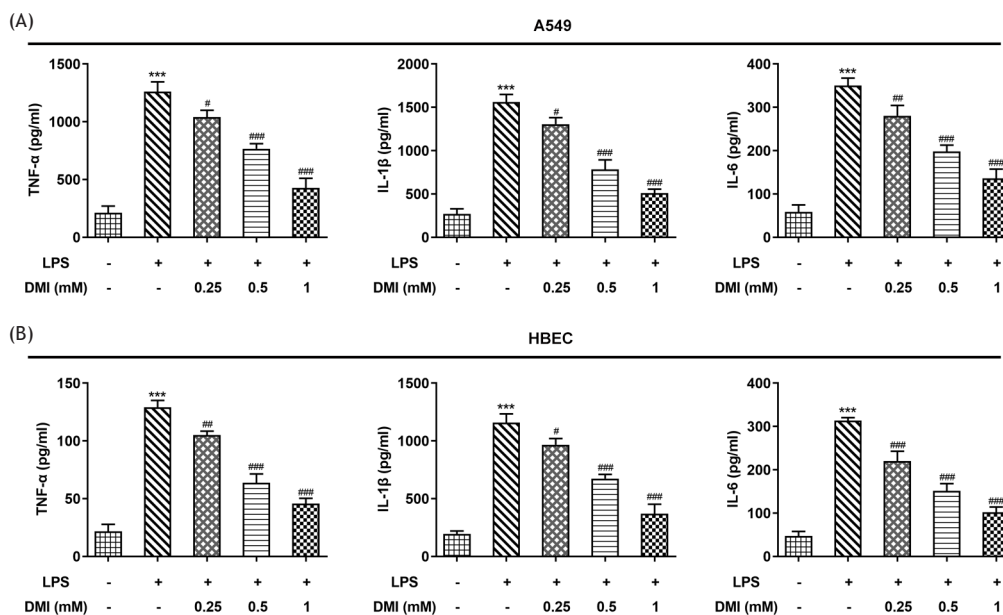


**Figure 2** DMI inhibits inflammatory release in LPS-induced A549 and HBEC cells. ELISA was performed to detect inflammatory factors, TNF- $\alpha$ , IL-1 $\beta$ , and IL-6 in the control, LPS-induced, and DMI-addition groups of (A) A549 and (B) HBEC cells. \*\*\*P < 0.001 vs. control; #P < 0.05, ##P < 0.01, and ###P < 0.001 vs. the LPS group.

### DMI increases the expression of pulmonary SP-A and SP-D in LPS-induced cells through regulating SIRT1 expression

The association between DMI and SIRT1 was determined using molecular docking. Hydrogen bonds (blue solid lines) were found to have formed between DMI and several amino acids of the protein, including SER-44, GLY-263, ARG-274, ALA-262, and PHE-273, which indicated that DMI may bind stably to SIRT1, as the atoms in DMI and the amino acids in SIRT1 protein formed hydrogen bonds, which are important intermolecular forces (Figures 4A and B). In order to verify that the aforementioned effects were caused by the activation of lung surfactants, Western blotting analysis was first used to detect the expression of lung surfactants in each group of epithelial cells. Compared with the control cells, expression levels of both SP-A and SP-D in the LPS-induced epithelial cells were significantly decreased, and the expression level was increased in a concentration-dependent manner following the addition of different DMI concentrations. Moreover, the expression level of SIRT1 was also determined using Western blotting analysis. SIRT1 expression was found to decrease in the LPS group relative to the control group but subsequently up-regulated after DMI treatment (Figures 4C and D). A SIRT1 inhibitor was then used to treat cells and its effect on SP-A and SP-D expression levels was determined using Western blotting analysis. The results revealed that treatment with SIRT1 inhibitor significantly suppressed SP-A and SP-D expression levels compared with the LPS + DMI (1 mM) group, suggesting that DMI may stimulate SP-A and SP-D expressions through SIRT1 (Figures 4E and F).

### SP-A and SP-D expression inhibition reverses the inhibitory effect of DMI on inflammatory release in LPS-induced cells

By constructing interference plasmids using shRNA, it was investigated whether the lung surfactant proteins mediated inflammatory release. RT-qPCR was first used to detect the level of interference. In both cell types, both SP-A and SP-D mRNA expression levels were significantly reduced compared with the shRNA-NC group, following transfection of the shRNA-SP-A-1/2 or shRNA-SP-D-1/2 plasmids, which indicated knockdown efficiency (Figures 5A and B). shRNA-SP-A-1 and shRNA-SP-D-1 were selected for subsequent experiments because of their greater interference efficiency. Next, ELISA was used to detect the levels of inflammatory factors. In order to determine expression differences in each group, an empty vector was transfected into LPS-induced cells treated with 1-mM DMI to act as an NC (LPS + DMI [1 mM] + shRNA-NC group). After silencing the expression of SP-A and SP-D (LPS + DMI [1 mM] + shRNA-SP-A group and LPS + DMI [1 mM] + shRNA-SP-D group), the levels of the measured inflammatory factors (TNF- $\alpha$ , IL-1 $\beta$ , and IL-6) were increased in both cell lines compared with the LPS + DMI (1 mM) + shRNA-NC group (Figures 5C and D). This indicated that both SP-A and SP-D might be involved in reducing inflammatory release in A549 and HBEC cells.

### SP-A and SP-D inhibition reverses the effect of DMI on cellular apoptosis

At the same time, both TUNEL staining and Western blotting analysis were used to detect the effect of SP-A and

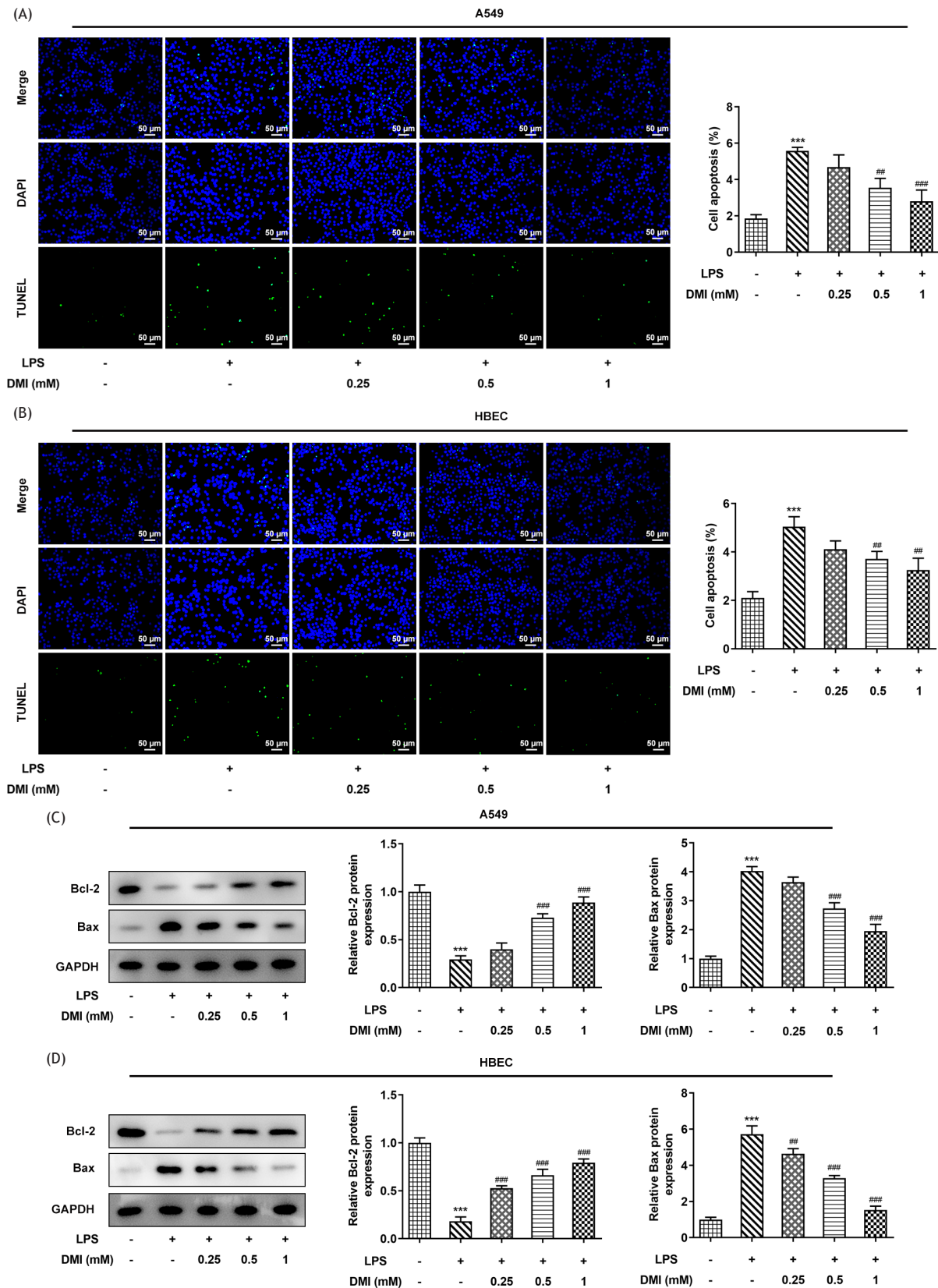


**Figure 3** DMI inhibits apoptosis in LPS-induced A549 and HBEC cells. TUNEL staining was used to detect (A) A549 and (B) HBEC cells apoptosis. DAPI stained all cells, while TUNEL stained apoptotic cells only. Magnification  $\times 200$ ; scale bar 50  $\mu\text{m}$ . Histogram depicts the apoptotic rate. Western blotting analysis was used to detect Bcl-2 and Bax expressions in (C) A549 and (D) HBEC cells. <sup>\*\*\*</sup> $P < 0.001$  vs. control; <sup>##</sup> $P < 0.01$  and <sup>###</sup> $P < 0.001$  vs. the LPS group.

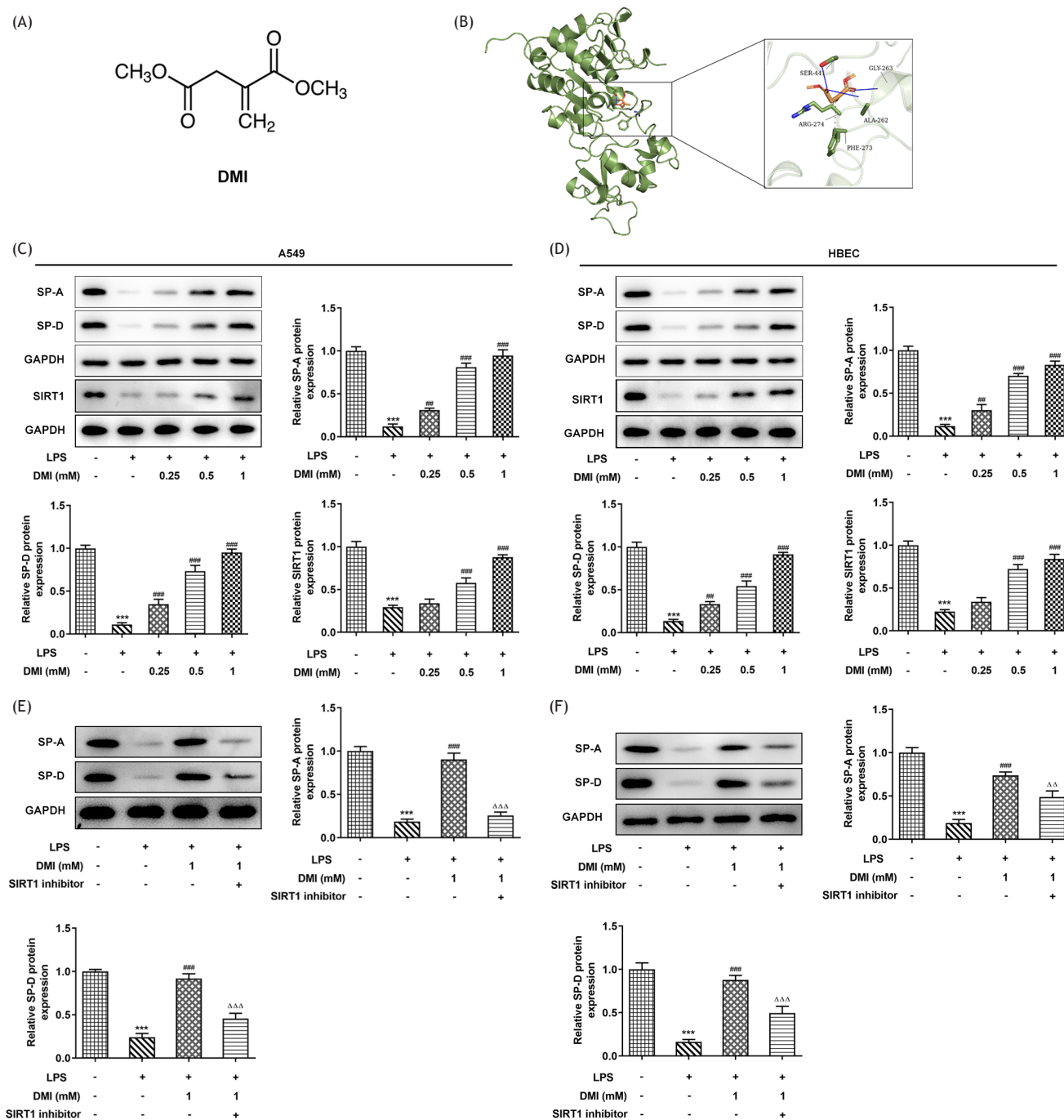


**Figure 4** DMI up-regulates the expressions of pulmonary SP-A and SP-D in LPS-induced cells by regulating SIRT1 expression. (A) Chemical structure of DMI. (B) Association between DMI and SIRT1 was determined using molecular docking. Western blotting analysis was used to detect the expressions of lung SP-A, SP-D, and SIRT1 in each group of (C) A549 and (D) HBEC cells. Effect of SIRT1 inhibitor on SP-A and SP-D expressions in (E) A549 and (F) HBEC cells was determined using Western blotting analysis. \*\*\*P < 0.001 vs. control; ##P < 0.01 and ###P < 0.001 vs. LPS group.  $\Delta\Delta$ P < 0.01 and  $\Delta\Delta\Delta$ P < 0.001 vs. the LPS + DMI (1 mM) group.

SP-D on cell apoptosis. The results of the TUNEL assay demonstrated that cell apoptosis was inhibited by addition of DMI (LPS + DMI [1 mM] group) compared with the LPS group; however, following SP-A or SP-D inhibition, cell apoptosis was promoted (Figures 6A and B). Furthermore, Bcl-2 expression was decreased and Bax expression was

increased after SP-A and SP-D inhibition compared with the LPS + DMI (1 mM) + shRNA-NC group, which also suggested the induction of cell apoptosis (Figures 6C and D). These results indicated that SP-A and SP-D may be involved in the underlying mechanism of the effects of DMI on cellular apoptosis.

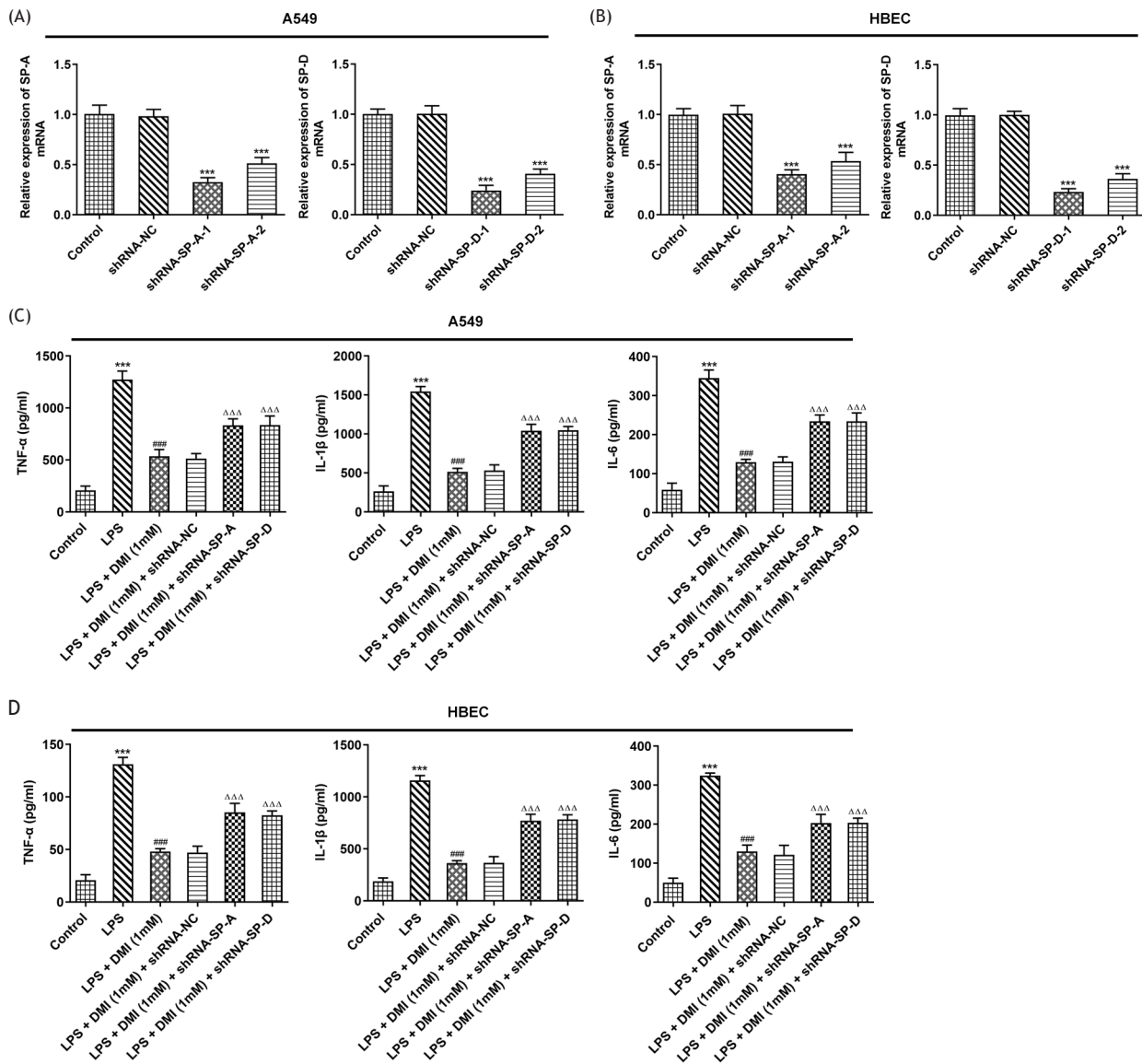


**Figure 5** SP-A and SP-D expression inhibition reverses the inhibitory effect of DMI on inflammatory release in LPS-induced cells. RT-qPCR was performed to detect the level of SP-A and SP-D interference in (A) A549 and (B) HBEC cells. ELISA was performed to detect the expression of inflammatory factors in (C) A549 and (D) HBEC cells. \*\*\* $P < 0.001$  vs. control; ### $P < 0.001$  vs. the LPS group; and  $\Delta\Delta\Delta P < 0.01$  vs. the LPS + DMI (1 mM) + shRNA-NC group.

## Discussion

Dimethyl itaconate is a derivative of itaconate, which is a metabolite produced in activated macrophages. Itaconate could regulate macrophage functioning<sup>23</sup> and exert anti-inflammatory effects by inhibiting the activity of succinate dehydrogenase.<sup>24</sup> Provided that DMI has been found to exert superior anti-inflammatory effects<sup>25</sup> and there is no evidence of its role in lung injury, the present study investigated the same effects. AT II cells are small cube-shaped cells that account for ~60% of alveolar epithelial cells. They can repair damaged alveoli following their differentiation into AT I cells. Another primary function of AT II cells is that they act as a source of pulmonary surfactants, which are lipoprotein complexes on the surface of

the alveoli. Lung surfactants can reduce surface tension at the air-water interface and stabilize the alveoli during exhalation. Surfactant deficiency or dysfunction has been linked to the occurrence and development of various lung diseases, such as ARDS, asthma, and chronic obstructive pulmonary disease (COPD).<sup>26</sup> A549 AT II cells and HBEC bronchial epithelial cells were selected in the present study. First, it was investigated whether DMI damages normal cells. DMI solution was serially diluted and added to the cells to detect impact on the survival rate of the two cell types. The results demonstrated that even the maximum tested concentration had no effect on the survival of either cell type. Therefore, it was added to the cells at the same time as LPS to determine its effect on the LPS-induced cell survival. In a previous study of DMI on

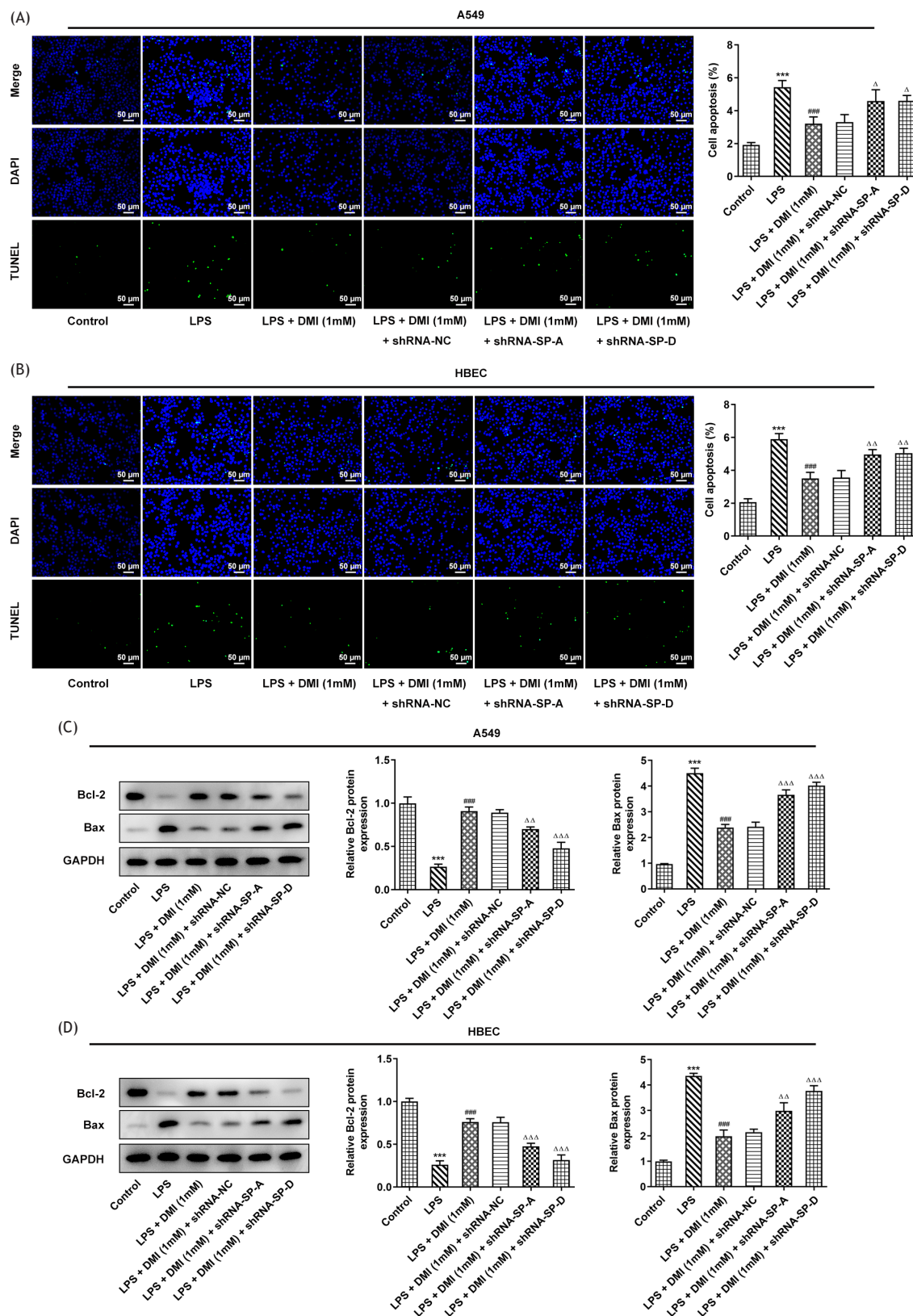


**Figure 6** SP-A and SP-D expression inhibition reverses the effect of DMI on cellular apoptosis. TUNEL staining was used to detect the effect of SP-A and SP-D knockdown on the apoptosis of (A) A549 and (B) HBEC cells. DAPI stained all cells, while TUNEL stained apoptotic cells only. Magnification  $\times 200$ ; scale bar 50  $\mu\text{m}$ . Histogram depicts the apoptotic rate. Western blotting analysis was used to detect Bcl-2 and Bax expressions in (C) A549 and (D) HBEC cells.  $***P < 0.001$  vs. the control;  $###P < 0.001$  vs. the LPS group;  $^{\Delta}P < 0.05$ ,  $^{\Delta\Delta}P < 0.01$ , and  $^{\Delta\Delta\Delta}P < 0.001$  vs. the LPS + DMI (1 mM) + shRNA-NC group.

the inflammatory response of macrophages, LPS was also used to induce a sepsis model, and it was found that it can inhibit the inflammatory response of macrophages.<sup>27</sup>

Cell damage can lead to inflammation and then apoptosis, so the effect of DMI on the inflammatory release and apoptosis of cells was studied. In total, three indicators, TNF- $\alpha$ , IL-1 $\beta$ , and IL-6, are commonly used to detect inflammatory release, of which TNF- $\alpha$  is a multidirectional pro-inflammatory cytokine secreted by a variety of cells, including macrophages, B cells, T cells, and fibroblasts. It plays an important role in the pathogenesis of septic shock, autoimmune diseases, rheumatoid arthritis, inflammation, and diabetes.<sup>28, 29</sup> IL-1 $\beta$  also can be secreted by a variety of cells, the most important of which are blood monocytes and macrophages. IL-1 $\beta$  is closely associated with the onset of gout and rheumatoid arthritis.<sup>30</sup> IL-6 plays a key role in acute inflammation and is associated with human metabolism and immune cell differentiation.<sup>31</sup> Examining inflammation by detecting the expression of these factors is common in research. The experimental results demonstrated that DMI effectively inhibits inflammation and apoptosis in induced cells, and promote the expression of lung SP-A, SP-D, and SIRT1. Surfactant proteins play a vital role in the normal functioning of lung tissue. Therefore, based on the current results, it was suggested that DMI could protect the lung to a certain extent.

As aforementioned, a previous study has revealed that SP-A and SP-D can maintain the integrity of epithelial cells while reducing inflammation in the lung.<sup>14</sup> Therefore, the hypothesis that SP-A and SP-D mediated the protective effect of DMI on the lung was proposed. Following *in silico* molecular docking, DMI was verified to bind to SIRT1. In addition, SIRT1 inhibitor could suppress the expression of SP-A and SP-D according to the results of Western blotting analysis. It was, therefore, confirmed that DMI affected SP-A and SP-D expressions through SIRT1. Subsequently, to determine whether SP-A and SP-D were involved in the inhibitory effect of DMI on cell inflammation and apoptosis, SP-A and SP-D interference plasmids were constructed. When SP-A and SP-D were silenced, the effects of DMI on cell inflammatory factors and apoptosis were reversed, which suggested that the effects of DMI were dependent on SP-A and SP-D. The present study indicated that DMI might suppress inflammation and cell apoptosis by activating SP-A and SP-D by regulating SIRT1 expression. Owing to the lack of other biological research on DMI and this study being limited to *in vitro* experiments, there is insufficient evidence to support the use of DMI as a drug candidate. Moreover, whether other signaling pathways are implicated remains to be explored. In-depth mechanistic studies of DMI in primary cells and an *in vivo* model are required and will be performed in the future studies. We hypothesize that DMI may have potential as a lead compound, and both DMI and its derivatives could become novel drugs for the treatment of lung injury.

## Conclusion

The findings of the present study revealed that DMI may inhibit inflammatory release and apoptosis in inflammatory cells. Following the silencing of SP-A and SP-D, the

inhibition of the protective effects of DMI on lung injury indicated that it could play a role in the disease by targeting SIRT1 and then activating SP-A and SP-D. The discovery of this pharmacological mechanism of DMI lays the foundation for its potential use in alleviating lung injury.

## Availability of Data and Materials

The datasets used and/or analyzed during the current study are available from the corresponding author on request.

## Author Contributions

Yun Shi designed and performed the experiments and made considerable contributions to the manuscript writing. Huaiqing Yin analyzed the data, contributed ideas, and revised the manuscript.

## Ethical Approval

Not applicable.

## Conflict of Interest

The authors declared that they had no competing interests.

## References

1. Vishnupriya S, Priya Dharshini LC, Sakthivel KM, Rasmi RR. Autophagy markers as mediators of lung injury—Implication for therapeutic intervention. *Life Sci.* 2020 Nov 1;260:118308. <https://doi.org/10.1016/j.lfs.2020.118308>
2. Nova Z, Skovierova H, Calkovska A. Alveolar-capillary membrane-related pulmonary cells as a target in endotoxin-induced acute lung injury. *Int J Mol Sci.* 2019 Feb 15;20(4):831. <https://doi.org/10.3390/ijms20040831>
3. Laubach VE, Sharma AK. Mechanisms of lung ischemia-reperfusion injury. *Curr Opin Organ Transplant.* 2016 Jun;21(3):246-52. <https://doi.org/10.1097/MOT.0000000000000304>
4. Hughes KT, Beasley MB. Pulmonary manifestations of acute lung injury: More than just diffuse alveolar damage. *Arch Pathol Lab Med.* 2017 Jul;141(7):916-22. <https://doi.org/10.5858/arpa.2016-0342-RA>
5. Shafeeq H, Lat I. Pharmacotherapy for acute respiratory distress syndrome. *Pharmacotherapy.* 2012 Oct;32(10):943-57. <https://doi.org/10.1002/j.1875-9114.2012.01115>
6. Matthay MA, Goolaerts A, Howard JP, Lee JW. Mesenchymal stem cells for acute lung injury: Preclinical evidence. *Crit Care Med.* 2010 Oct;38(10 Suppl):S569-73. <https://doi.org/10.1097/CCM.0b013e3181f1ff1d>
7. Beitler JR, Malhotra A, Thompson BT. Ventilator-induced lung injury. *Clin Chest Med.* 2016 Dec;37(4):633-46. <https://doi.org/10.1016/j.ccm.2016.07.004>
8. Katira BH. Ventilator-induced lung injury: Classic and novel concepts. *Respir Care.* 2019 Jun;64(6):629-37. <https://doi.org/10.4187/respcare.07055>
9. Hanania AN, Mainwaring W, Ghebre YT, Hanania NA, Ludwig M. Radiation-induced lung injury: Assessment and management. *Chest.* 2019 Jul;156(1):150-62. <https://doi.org/10.1016/j.chest.2019.03.033>

10. Monsel A, Zhu YG, Gudapati V, Lim H, Lee JW. Mesenchymal stem cell-derived secretome and extracellular vesicles for acute lung injury and other inflammatory lung diseases. *Expert Opin Biol Ther.* 2016 Jul;16(7):859-71. <https://doi.org/10.1517/14712598.2016.1170804>
11. Kishore U, Greenhough TJ, Waters P, Shrive AK, Ghai R, Kamran MF, et al. Surfactant proteins SP-A and SP-D: Structure, function and receptors. *Mol Immunol.* 2006 Mar;43(9):1293-315. <https://doi.org/10.1016/j.molimm.2005.08.004>
12. Wu A, Song H. Regulation of alveolar type 2 stem/progenitor cells in lung injury and regeneration. *Acta Biochim et Biophys Sinica.* 2020 Jul 10;52(7):716-22. <https://doi.org/10.1093/abbs/gmaa052>
13. Schicht M, Knipping S, Hirt R, Beileke S, Sel S, Paulsen F, et al. Detection of surfactant proteins A, B, C, and D in human nasal mucosa and their regulation in chronic rhinosinusitis with polyps. *Am J Rhinol Allergy.* 2013 Jan;27(1):24-9. <https://doi.org/10.2500/ajra.2013.27.3838>
14. Goto H, Ledford JG, Mukherjee S, Noble PW, Williams KL, Wright JR. The role of surfactant protein A in bleomycin-induced acute lung injury. *Am J Respir Crit Care Med.* 2010 Jun 15;181(12):1336-44. <https://doi.org/10.1164/rccm.200907-1002OC>
15. Gu C, Zhang Q, Ni D, Xiao QF, Cao LF, Fei CY, et al. Therapeutic effects of SRT2104 on lung injury in rats with emphysema via reduction of type II alveolar epithelial cell senescence. *Copd.* 2020 Aug;17(4):444-51. <https://doi.org/10.1080/15412555.2020.1797657>
16. Gu L, Lin J, Wang Q, Li C, Peng X, Fan Y, et al. Dimethyl itaconate protects against fungal keratitis by activating the Nrf2/HO-1 signaling pathway. *Immunol Cell Biol.* 2020 Mar;98(3):229-41. <https://doi.org/10.1111/imcb.12316>
17. Zhang D, Lu Z, Zhang Z, Man J, Guo R, Liu C, et al. A likely protective effect of dimethyl itaconate on cerebral ischemia/reperfusion injury. *Int Immunopharmacol.* 2019 Dec;77:105924. <https://doi.org/10.1016/j.intimp.2019.105924>
18. Zhao C, Jiang P, He Z, Yuan X, Guo J, Li Y, et al. Dimethyl itaconate protects against lipopolysacchride-induced mastitis in mice by activating MAPKs and Nrf2 and inhibiting NF- $\kappa$ B signaling pathways. *Microb Pathog.* 2019 Aug;133:103541. <https://doi.org/10.1016/j.micpath.2019.05.024>
19. Pflanzgraff A, Weindl G. Intracellular lipopolysaccharide sensing as a potential therapeutic target for sepsis. *Trends Pharmacol Sci.* 2019 Mar;40(3):187-97. <https://doi.org/10.1016/j.tips.2019.01.001>
20. Zhang C, Zhu X, Hua Y, Zhao Q, Wang K, Zhen L, et al. YY1 mediates TGF- $\beta$ 1-induced EMT and pro-fibrogenesis in alveolar epithelial cells. *Respir Res.* 2019 Nov 8;20(1):249. <https://doi.org/10.1186/s12931-019-1223-7>
21. Pal PB, Sonowal H, Shukla K, Srivastava SK, Ramana KV. Aldose reductase regulates hyperglycemia-induced HUVEC death via SIRT1/AMPK- $\alpha$ 1/mTOR pathway. *J Mol Endocrinol.* 2019 Jul 1;63(1):11-25. <https://doi.org/10.1530/JME-19-0080>
22. Livak KJ, Schmittgen TD. Analysis of relative gene expression data using real-time quantitative PCR and the 2(-delta delta C(T)) method. *Methods (San Diego).* 2001 Dec;25(4):402-8. <https://doi.org/10.1006/meth.2001.1262>
23. Mills EL, Ryan DG, Prag HA, Dikovskaya D, Menon D, Zaslona Z, et al. Itaconate is an anti-inflammatory metabolite that activates Nrf2 via alkylation of KEAP1. *Nature.* 2018 Apr 5;556(7699):113-7. <https://doi.org/10.1038/nature25986>
24. Domínguez-Andrés J, Novakovic B, Li Y, Scicluna BP, Gresnigt MS, Arts RJW, et al. The itaconate pathway is a central regulatory node linking innate immune tolerance and trained immunity. *Cell Metab.* 2019 Jan 8;29(1):211-20.e5. <https://doi.org/10.1016/j.cmet.2018.09.003>
25. Swain A, Bambouskova M, Kim H, Andhey PS, Duncan D, Auclair K, et al. Comparative evaluation of itaconate and its derivatives reveals divergent inflammasome and type I interferon regulation in macrophages. *Nature Metab.* 2020 Jun;2(7):594-602. <https://doi.org/10.1038/s42255-020-0210-0>
26. Shen L, Li L, She H, Yue S, Li C, Luo Z. Inhibition of pulmonary surfactants synthesis during N-methyl-D-aspartate-induced lung injury. *Basic Clin Pharmacol Toxicol.* 2010 Sep;107(3):751-7. <https://doi.org/10.1111/j.1742-7843.2010.00572.x>
27. Zhang S, Jiao Y, Li C, Liang X, Jia H, Nie Z, et al. Dimethyl itaconate alleviates the inflammatory responses of macrophages in sepsis. *Inflammation.* 2021 Apr;44(2):549-57. <https://doi.org/10.1007/s10753-020-01352-4>
28. Akash MSH, Rehman K, Liaqat A. Tumor necrosis factor-alpha: Role in development of insulin resistance and pathogenesis of type 2 diabetes mellitus. *J Cell Biochem.* 2018 Jan;119(1):105-10. <https://doi.org/10.1002/jcb.26174>
29. Holtmann MH, Neurath MF. Differential TNF-signaling in chronic inflammatory disorders. *Curr Mol Med.* 2004 Jun;4(4):439-44. <https://doi.org/10.2174/1566524043360636>
30. Jia P, Liu W, Liu S, Gao W. Therapeutic effects of Hedyotis diffusa Willd. on type II collagen-induced rheumatoid arthritis in rats. *Chin J Appl Physiol (Zhongguo Ying Yong Sheng Li Xue Za Zhi).* 2018 Jun 8;34(6):558-61.
31. Kang S, Tanaka T, Narazaki M, Kishimoto T. Targeting interleukin-6 signaling in clinic. *Immunity.* 2019 Apr 16;50(4):1007-23. <https://doi.org/10.1016/j.immuni.2019.03.026>